

Supporting Information for:

The $\text{Ba}_3\text{Mo}_{1-x}\text{W}_x\text{NbO}_{8.5}$ ion conductor: Insights on local Coordination from X-ray and Neutron Total Scattering

M. Coduri^{1,*}, A. Bernasconi¹, H. Fischer², L. Malavasi^{1,*}

¹ University of Pavia, Chemistry department, via Taramelli 16, 27100, Pavia (PV), Italy

² Institut Laue Langevin, 9 rue Horowitz, 38100, Grenoble, France

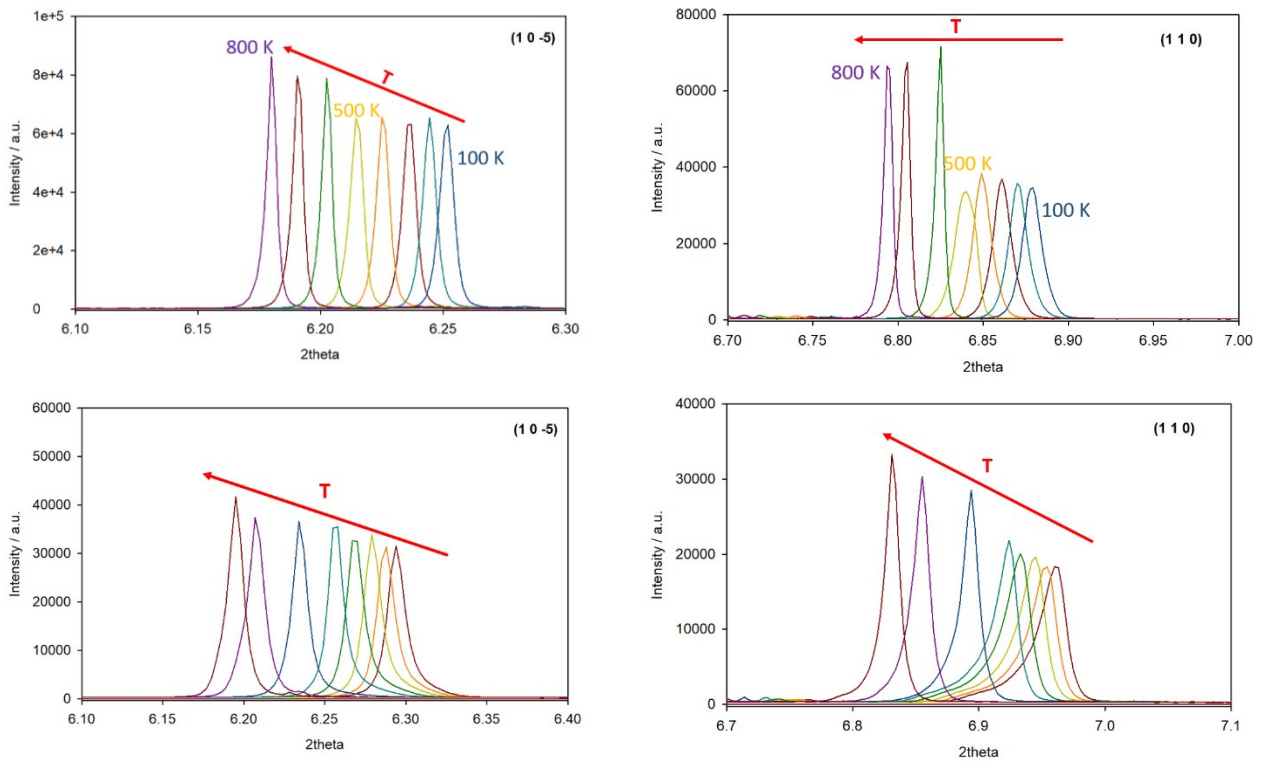


Figure S1: Temperature evolution from 100 to 800 K of experimental XRPD data of (top) $\text{Ba}_3\text{MoNbO}_{8.5}$ and (bottom) $\text{Ba}_3\text{WNbO}_{8.5}$. Left: (10-5) reflection, right: (110) reflection.

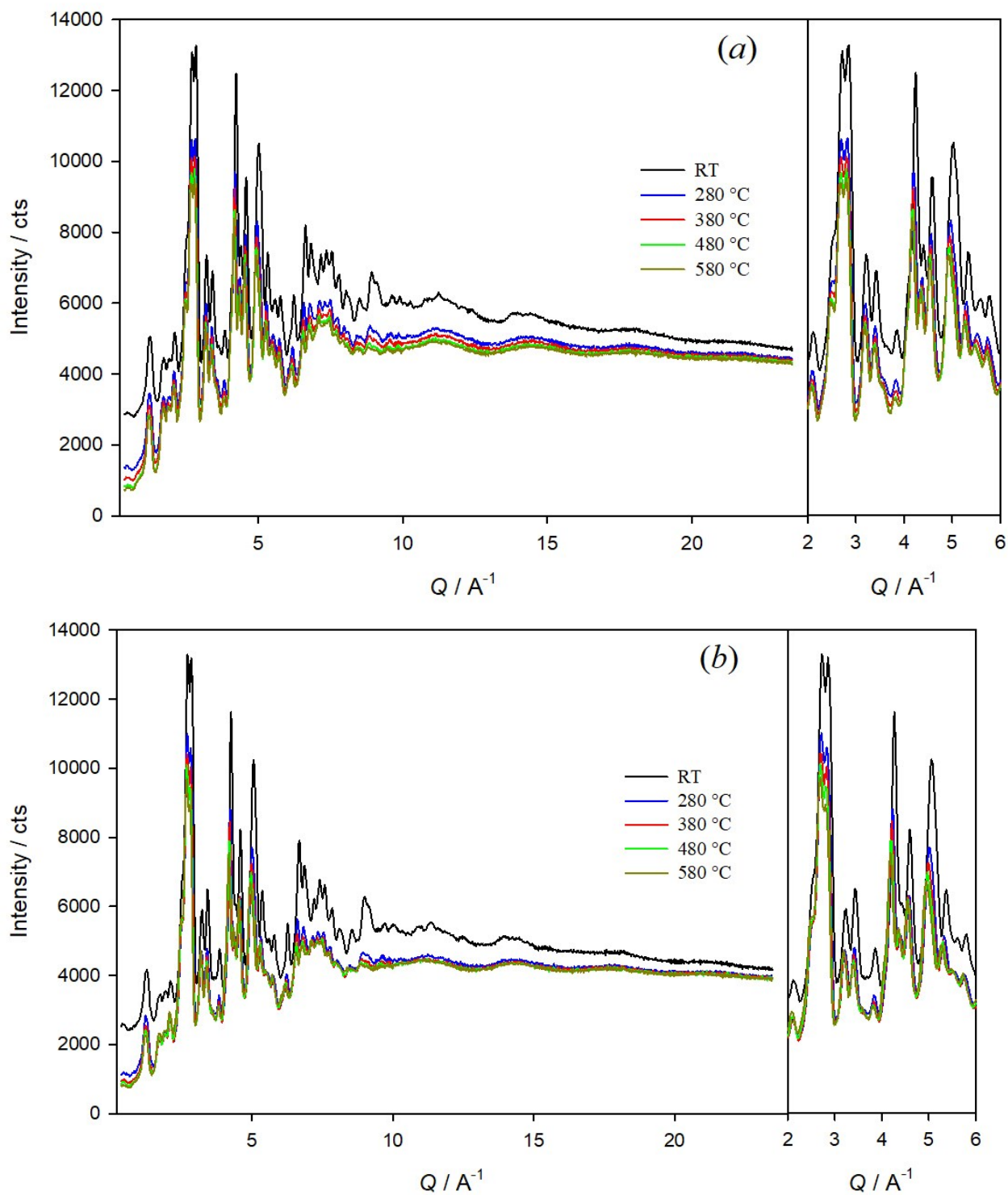


Figure S2: Experimental NDP patterns before Fourier Transform for (a) $\text{Ba}_3\text{MoNbO}_{8.5}$ and (b) $\text{Ba}_3\text{WNbO}_{8.5}$. The right panel highlights the main peaks at low angle. No peculiar effect is observed on Bragg peaks after 300 °C, likely because of the limited resolution of the instrument.

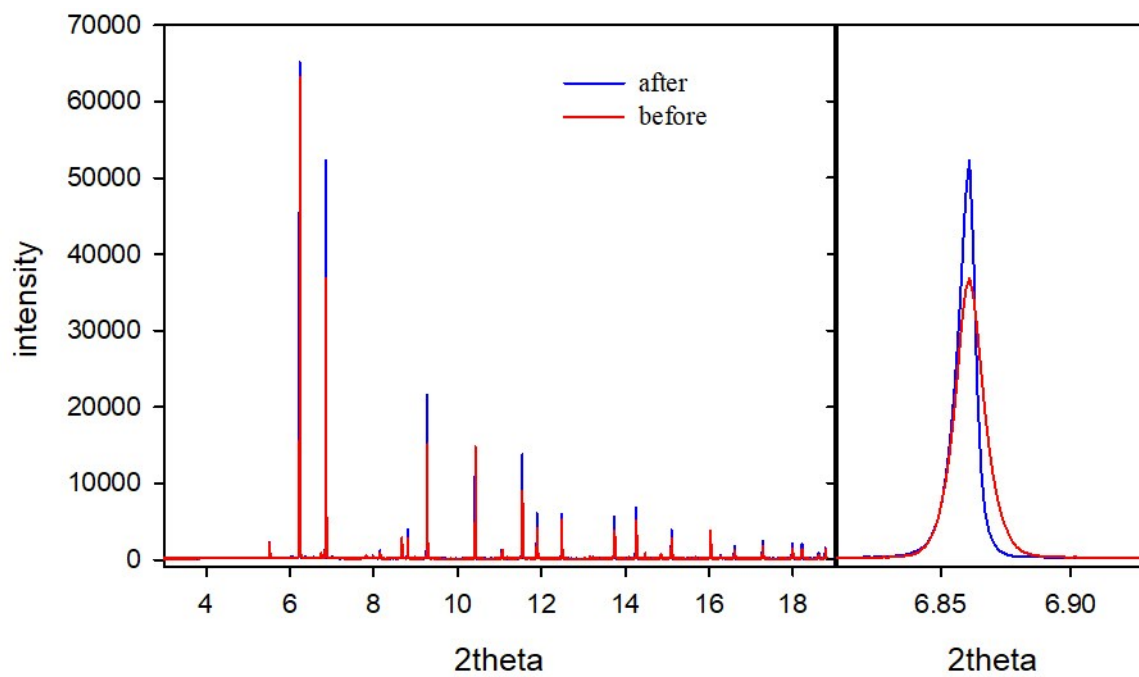


Figure S3: Experimental XRPD patterns of Ba₃MoNbO_{8.5} collected at room temperature before (red) and after (blue) heating up to 650 °C.

Table S1. Structural parameters computed by Rietveld refinements for Ba₃WNbO_{8.5}, space group *R-3m*. The temperature is in °C unit, lattice parameters in Å, displacement parameters in Å².

<i>T</i>	27	127	227	327	427	527	627
<i>a</i>	5.85619(8)	5.86560(3)	5.87305(8)	5.89639(5)	5.92966(5)	5.94957(4)	5.96889(5)
<i>c</i>	21.0111(4)	21.0474(4)	21.0964(3)	21.1659(2)	21.2398(2)	21.2637(2)	21.2756(2)
U ₁₁ (Ba1)	0.0093(15)	0.009(2)	0.018(2)	0.027(2)	0.039(2)	0.040(2)	0.048(2)
U ₃₃ (Ba1)	0.029(2)	0.032(2)	0.036(2)	0.044(2)	0.043(2)	0.041(2)	0.039(3)
U ₁₂ (Ba1)	0.0047(7)	0.0047(8)	0.0092(9)	0.0135(8)	0.0196(9)	0.020(1)	0.024(1)
z(Ba2)	0.2103(1)	0.2102(1)	0.2104(1)	0.20929(9)	0.2074(1)	0.2072(1)	0.2072(1)
U ₁₁ (Ba2)	0.016(1)	0.017(1)	0.019(1)	0.019(3)	0.022(1)	0.027(1)	0.032(1)
U ₃₃ (Ba2)	0.032(2)	0.033(2)	0.039(2)	0.057(2)	0.075(2)	0.076(2)	0.072(2)
U ₁₂ (Ba2)	0.0080(5)	0.0086(5)	0.0095(5)	0.0096(4)	0.0113(4)	0.0134(5)	0.0158(6)
z(M1)	0.3941(1)	0.3941(1)	0.3937(1)	0.39471(8)	0.3970(1)	0.3976(1)	0.3978(1)
U(M1)	0.0112(7)	0.0133(7)	0.0148(8)	0.0153(4)	0.0170(5)	0.0213(3)	0.0248(6)
<i>o.f.</i> (M1)	0.830(2)	0.830(2)	0.834(2)	0.832(2)	0.880(2)	0.912(2)	0.927(2)
z(M2)	0.5212(3)	0.5208(3)	0.5199(4)	0.5195(3)	0.5194(4)	0.5189(6)	0.5184(9)
U(M2)	0.0093(7)	0.0114(7)	0.0128(8)	0.0133(5)	0.0150(5)	0.0193(5)	0.0228(6)
<i>o.f.</i> (M2)	0.170	0.170	0.166	0.168	0.120	0.088	0.073
x(O1)	0.1821(8)	0.1837(9)	0.1835(9)	0.1821(7)	0.1799(6)	0.1816(6)	0.1820(7)
z(O1)	0.1077(4)	0.1079(4)	0.1076(4)	0.1067(3)	0.1039(3)	0.1036(3)	0.1027(4)
U(O1)	0.016(2)	0.019(2)	0.021(2)	0.030(2)	0.038(2)	0.042(2)	0.046(3)
<i>o.f.</i> (O2)	0.833	0.833	0.833	0.0813(15)	0.0659(14)	0.0568(13)	0.0531(18)
x(O3)	-	-	-	0.098*	0.098*	0.09(2)	0.08(2)
z(O3)	-	-	-	0.324*	0.324*	0.327(2)	0.329(3)
<i>o.f.</i> (O3)	0	0	0	0.006(8)	0.078(7)	0.120(7)	0.134(7)
O per formula	8.5	8.5	8.5	8.475	8.45	8.425	8.40
Rwp	15.43	15.21	16.04	11.61	10.46	10.21	10.88
Rp	10.28	10.10	10.56	7.92	7.61	7.37	7.33

* fixed from ref. [14].

Table S2. Structural parameters computed by Rietveld refinements for Ba₃MoNbO_{8.5}, space group *R-3m*. The temperature is in °C unit, lattice parameters in Å, displacement parameters in Å².

<i>T</i>	27	127	227	327	427	527	627
<i>a</i>	5.92289(2)	5.93298(2)	5.94164(3)	5.95481(1)	5.97218(2)	5.98118(2)	5.98059(2)
<i>c</i>	21.09167(9)	21.12771(8)	21.1673(1)	21.20494(6)	21.23104(6)	21.2707(1)	21.3371(1)
U ₁₁ (Ba1)	0.018(1)	0.020(1)	0.024(1)	0.034(1)	0.040(1)	0.047(2)	0.046(2)
U ₃₃ (Ba1)	0.034(1)	0.034(1)	0.038(1)	0.034(1)	0.035(1)	0.041(2)	0.047(4)
U ₁₂ (Ba1)	0.0092(6)	0.0099(6)	0.0119(6)	0.0172(5)	0.0199(5)	0.0233(8)	0.0228(9)
z(Ba2)	0.20748(7)	0.20736(4)	0.20753(6)	0.20734(5)	0.20681(6)	0.20682(9)	0.2068(1)
U ₁₁ (Ba2)	0.0108(6)	0.0157(8)	0.0188(7)	0.0248(5)	0.0300(6)	0.035(1)	0.046(1)
U ₃₃ (Ba2)	0.056(1)	0.065(1)	0.072(1)	0.066(1)	0.075(1)	0.086(2)	0.101(3)
U ₁₂ (Ba2)	0.0054(3)	0.0079(5)	0.0094(4)	0.00124(3)	0.00150(3)	0.00174(5)	0.00228(7)
z(M1)	0.3981(1)	0.3985(1)	0.3984(1)	0.3985(1)	0.3991(1)	0.3989(1)	0.3994(2)
U(M1)	0.0138(6)	0.0150(6)	0.0170(5)	0.0199(4)	0.0213(5)	0.0230(6)	0.0249(7)
<i>o.f.</i> (M1)	0.900(2)	0.906(2)	0.900(2)	0.910(2)	0.926(2)	0.932(2)	0.938(2)
z(M2)	0.5196(7)	0.5186(6)	0.5182(6)	0.5169(6)	0.5167(7)	0.5169(10)	0.517(1)
U(M2)	0.0138*	0.0150*	0.0170*	0.0125(4)	0.0126(6)	0.0127(8)	0.14(1)
<i>o.f.</i> (M2)	0.100	0.094	0.100	0.090	0.074	0.068	0.62
x(O1)	0.1758(7)	0.1765(6)	0.1763(6)	0.1768(5)	0.1769(5)	0.1766(9)	0.1788(7)
z(O1)	0.1040(3)	0.1019(3)	0.1019(3)	0.1025(2)	0.1024(2)	0.1031(4)	0.1020(4)
U(O1)	0.024(2)	0.032(2)	0.032(2)	0.037(2)	0.043(2)	0.048(2)	0.042(2)
<i>o.f.</i> (O2)	0.426(9)	0.415(11)	0.410(11)	0.411(9)	0.397(9)	0.395(12)	0.397(14)
x(O3)	0.073(6)	0.068(7)	0.082(6)	0.063(6)	0.054(8)	0.051(9)	0.057(11)
z(O3)	0.332(1)	0.329(1)	0.331(1)	0.3273(8)	0.3285(8)	0.3287(9)	0.327(1)
<i>o.f.</i> (O3)	0.204(5)	0.209(6)	0.212(6)	0.207(5)	0.210(5)	0.207(6)	0.205(7)
O per formula	8.5	8.5	8.5	8.475	8.45	8.425	8.40
Rwp	14.59	12.55	14.76	12.85	12.72	18.60	18.08
Rp	10.21	8.80	10.82	9.48	9.38	14.72	14.05

* constrained to the same value as the M1 cation.

The refinements were performed by imposing a progressive O non stoichiometry as described in the main text. All displacement parameters were treated isotropically but for Ba sites, which showed marked anisotropy at all temperatures. The values for O sites were constrained to be the same to avoid correlations with site fractions and facilitate fit convergence. We associate the higher residuals to problems refining the line profile, especially when strongly anisotropic. Concerning Ba₃WNbO_{8.5}, for low temperature data, the O2-O3 occupancies were set to guarantee full occupation of the O2, otherwise slightly negative values for O3 were obtained. When the O3 site fraction was less than 0.1, its atomic coordinates were set to the values obtained from single crystal [14] and not refined, while they were refined for the highest temperatures of the investigation.

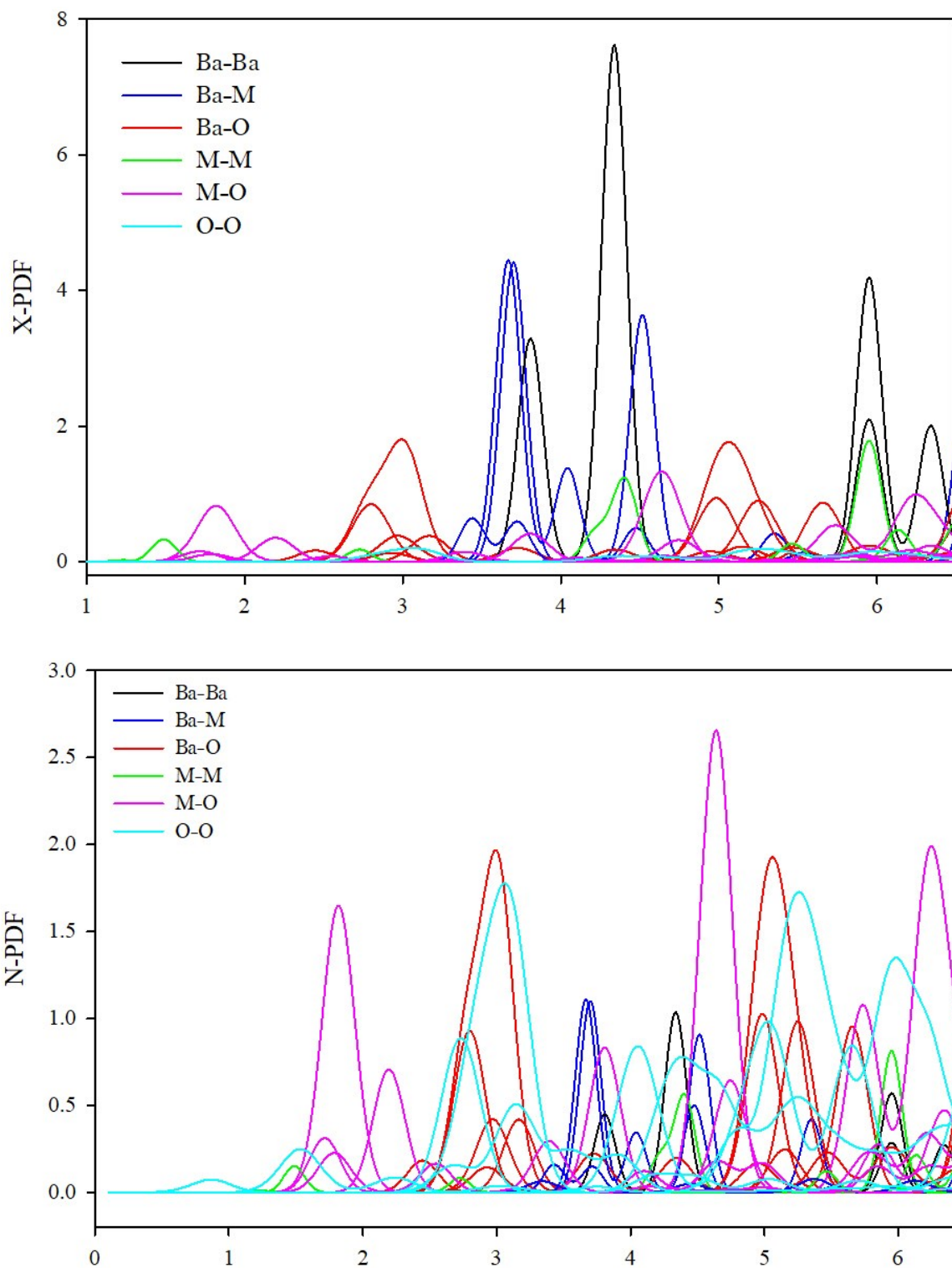


Figure S4. (top) X-ray and (bottom) neutron partial PDF calculated for $\text{Ba}_3\text{MoNbO}_{8.5}$. The background slope $-4\pi\rho_0r$ was subtracted to facilitate comparisons. The different peaks associated to the same colours indicate different crystallographic sites involving the same elements, *e.g.* the Ba-O (red) pairs includes Ba1-O1, Ba1-O2, Ba1-O3, Ba2-O1, Ba2-O2 and Ba2-O3 contributions.

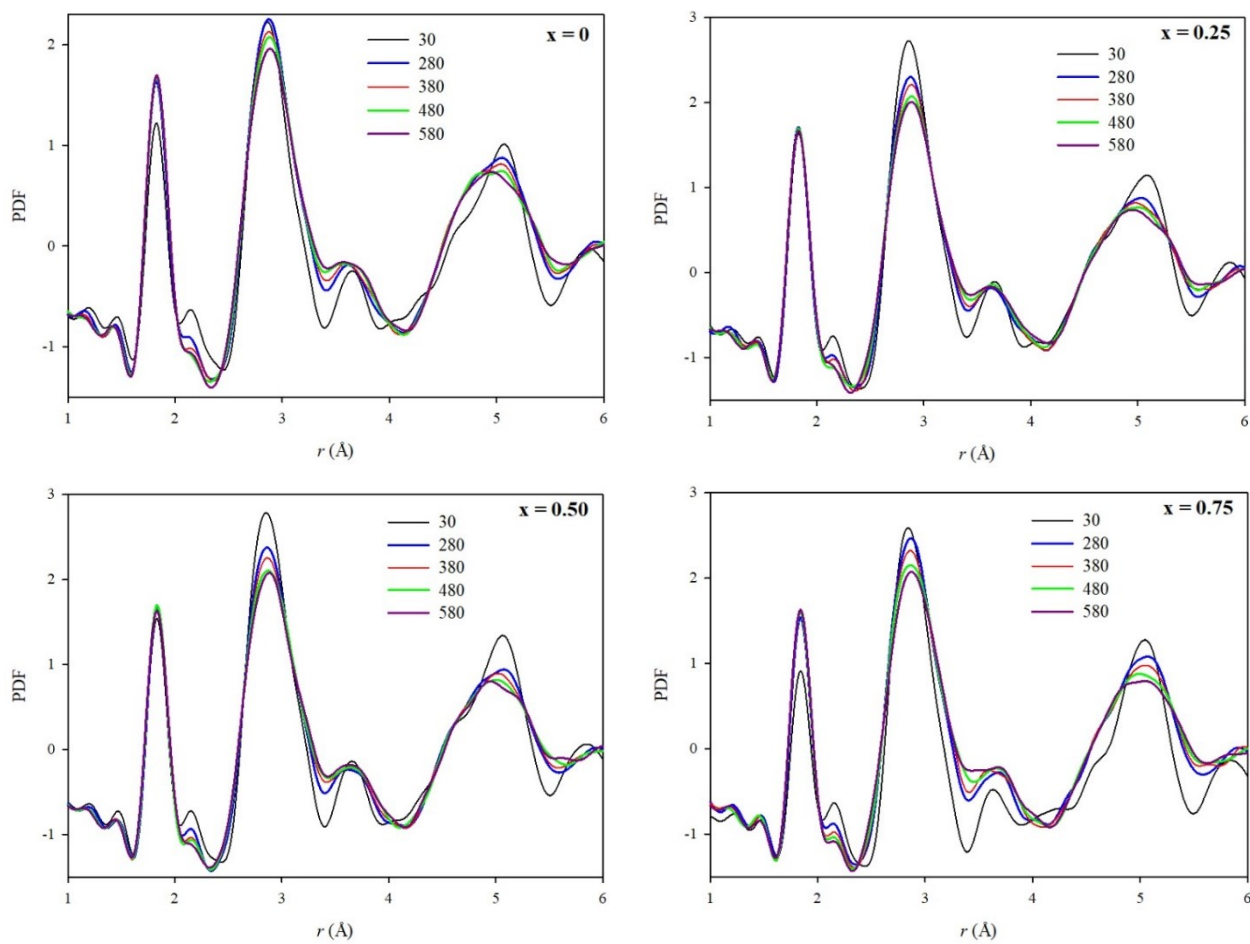


Figure S5. Temperature resolved experimental N-PDF curves for all the compositions investigated (W end member reported in the main text).

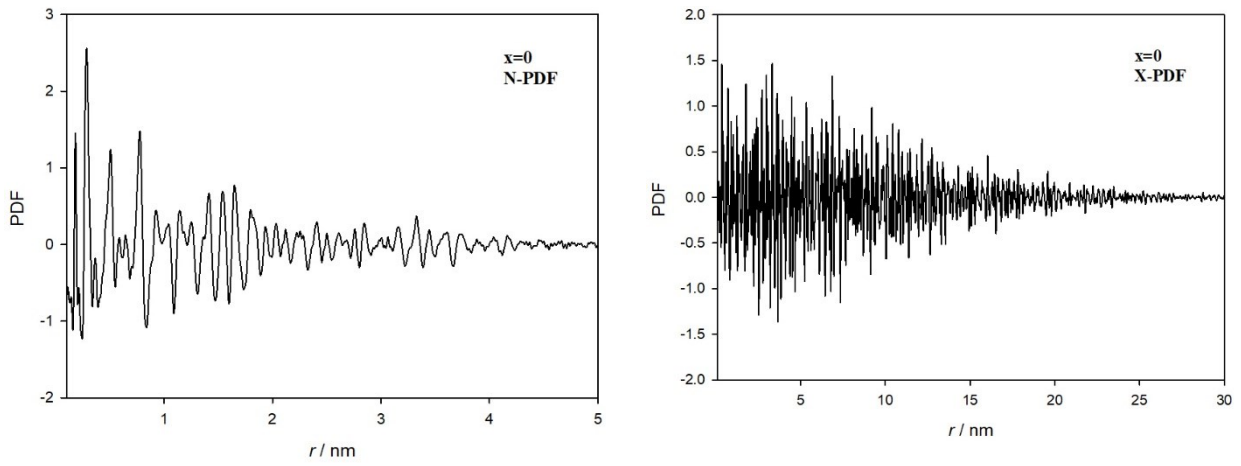


Figure S6: Full interatomic distance range of experimental neutron (left) and X-ray (right) PDF for specimen $\text{Ba}_3\text{MoNbO}_{8.5}$.

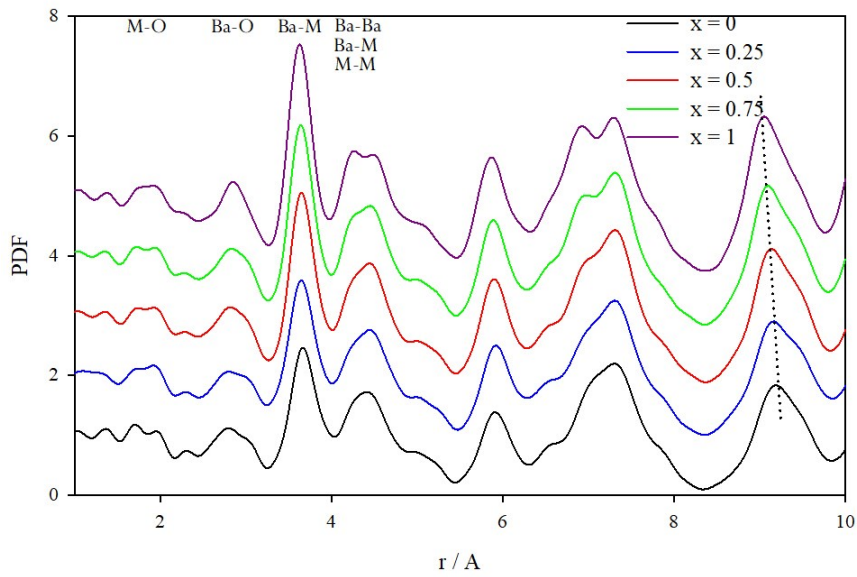


Figure S7. Experimental X-PDF at RT as a function of the W/Mo composition.

Text S1: *estimate of M-O(V) distances*

A first estimate of interatomic distances is provided by summing the O and M crystal radii. As for Mo⁺⁶, this leads to 1.76, 1.85 and 1.94 Å for IV, V and VI coordination. The same is observed for W, while Nb⁺⁵ shows larger values by 0.05 Å.

Another approach to estimate the interatomic distance is the BVS, assuming that Mo valence is 6 and the coordination undistorted. A valence equal to 6 is obtained with 4 Mo-O pairs at 1.76 Å, 5 pairs at 1.84 Å and 6 pairs at 1.91 Å. The latter is, however, much shorter than the distance observed experimentally by Rietveld and PDF analysis, i.e. 2.20 Å. The reason for the discrepancy is that the coordination is strongly distorted, with three shorter and three longer distances. Assuming the short distances are the same as the tetrahedral coordination, mostly defined by the position of O1, a valence 6 is obtained by adding three Mo-O pairs at 2.16 Å. Similarly, for a 5-fold coordination, one obtains an ideal coordination composed of 5 pairs lying at 1.84 Å, or three short (1.76 Å) and two long (2.01 Å) pairs.

According to this model, the 5-fold coordinated Mo-O should occur at ~2.0 Å, where a minimum in the N-PDF peaks is generally observed.

Concerning comparisons with literature, we exploited the database given by ref 29 of the main text (Waroquiers et al., Chem Mater 2017, 29, 19, 8346-8360), which filters all entries in inorganic crystallographic database according to the different coordination and valence of each element. Among the entries related to 5-fold coordinated Mo⁺⁶ ions, many are actually 4-fold coordinated (e.g. CdMoO₄, MoPbO₄, FeMoVO₇, BaBi₁₂Mo₄WO₃₄ and others) and most of structures reported are monoclinic or triclinic and display a broad distribution of interatomic distances, often ranging from 1.7 to more than 2.0 Å, see for example:

K₂Mo₃O₁₀: C2/c, Mo-O distances: 1.64, 1.70, 1.90, 1.95, 2.08 Å

Y₂MoO₆: C2/c, Mo-O distances: 1.79, 1.79, 1.80, 1.81, 2.21

ZrMo₂O₈: C2/c, Mo-O distances: 1.68, 1.76, 1.86, 1.99, 2.04

La₄Cu₃MoO₁₂: P2₁/m, Mo-O distances: 1.81, 1.83, 1.84, 2x1.88

LaMoBO₆: P2₁/c, Mo-O distances: (1.74, 1.74, 1.79, 1.83, 2.44)x2

This suggests that the occurrence of Mo-O(V) would likely introduce a broad distribution of interatomic distances, leading to a blurred signal in the PDF rather than a peak, making this coordination hard to detect from PDF.

Text S2: PDF modelling

Figure S6 reports the HA model refined against the RT N-PDF of $\text{Ba}_3\text{MoNbO}_{8.5}$. A nice fit ($R_w=0.07$) is obtained by using large displacement parameters (unphysical), but excluding the first neighbour pairs, which are much sharper.

This is consistent with the presence of well-ordered M-O polyhedra, which, however, are stacked in a disordered way. Therefore, the application of the same model to the local scale leads to an unreliable fit because of the different PDF peak profiles. A fit accounting for both the first neighbours and larger interatomic distances can be performed only using a bigger box approach, as the one by Chambers *et al.* [17]

We did not proceed with the two-phase modelling of N-PDF as the single HA already worked well. This is a similar effect as the high temperature X-PDF, where the two-phase modelling proved to be unreliable for the same reason.

Therefore, our approach towards PDF investigation has been the following:

- extract information about coordination from direct analysis of N-PDF peaks (we chose neutrons as they provide much better contrast to O ions)
- investigate the structure on the nanometre scale from refinement of X-PDF, which, having less peak overlap, allows to resolve the structural motif.

Another issue related to the modelling of N-PDF data is that, due to the limited Q -space resolution, PDF data extended up only to ~ 4 nanometres (Figure S6), with a consequent peak broadening increasing with r .

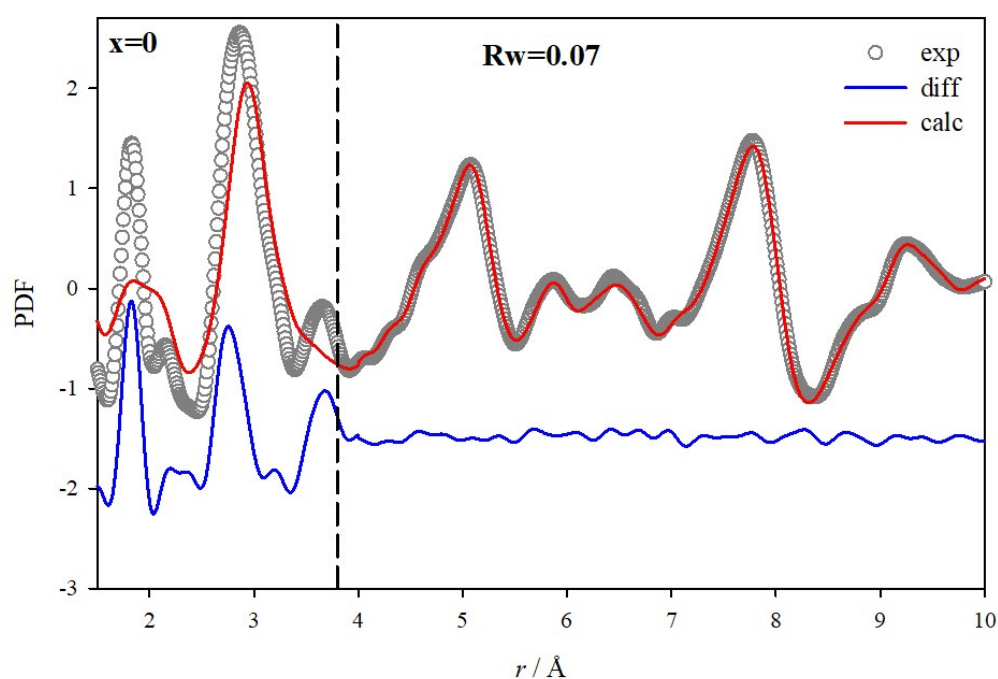


Figure S8. Application of the long range HA model, refined in the right hand part, to the very local scale. Although a parameter for accounting for correlated motion has been refined, the peaks are too sharp to be accounted for by the HA model.

A further attempt to process N-PDF data was performed by allowing the local formation of distorted polyhedra with coordination 5. We implemented the model as follows: we selected a M1 octahedron and allowed the O2 ions connecting the nearby octahedra to relax in the direction of the adjacent O3 site, which was allowed to move as well in the same direction, away from the O2 site. The shift of the O3 site was constrained to be larger than that of the O2 site, otherwise the corresponding interatomic distance would be too short. This has been implemented in a 2 x 2 x 1 supercell in order to be able to deal with independent polyhedra, which would be otherwise equivalent for translation symmetry. The O sites not involved in the distortion were considered to be partially occupied as in the average hybrid model.

We first applied the model in the interatomic distance range from 1.5 to 10 Å. The fit quality is very similar to the hybrid HA model.

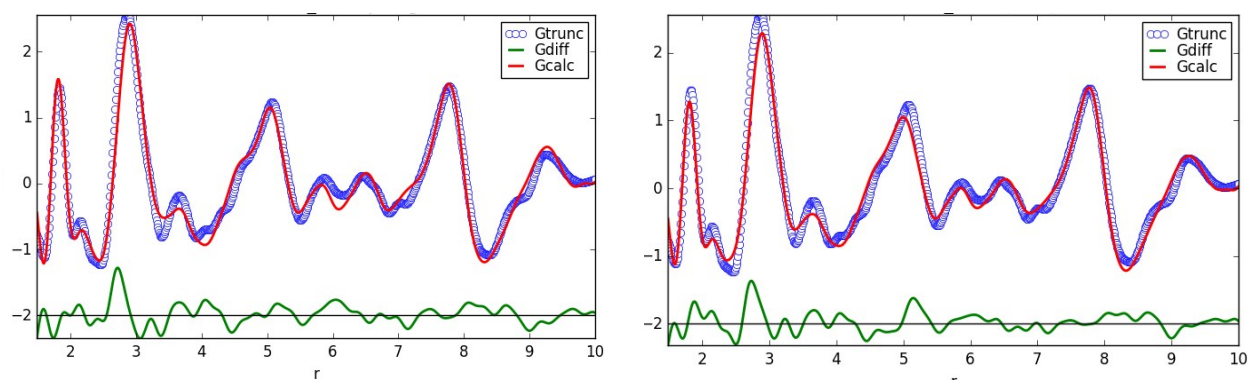


Figure S9. PDF modelling up to 10 Å using the hybrid model (left, $R_w=0.21$) and allowing the O displacement to form 5-fold coordinated M1 polyhedra (right, $R_w=0.20$)

As discussed already, one of the issues of the refinement is to account for both rigid units and their disordered stacking. Then we applied the same models to the local scale:

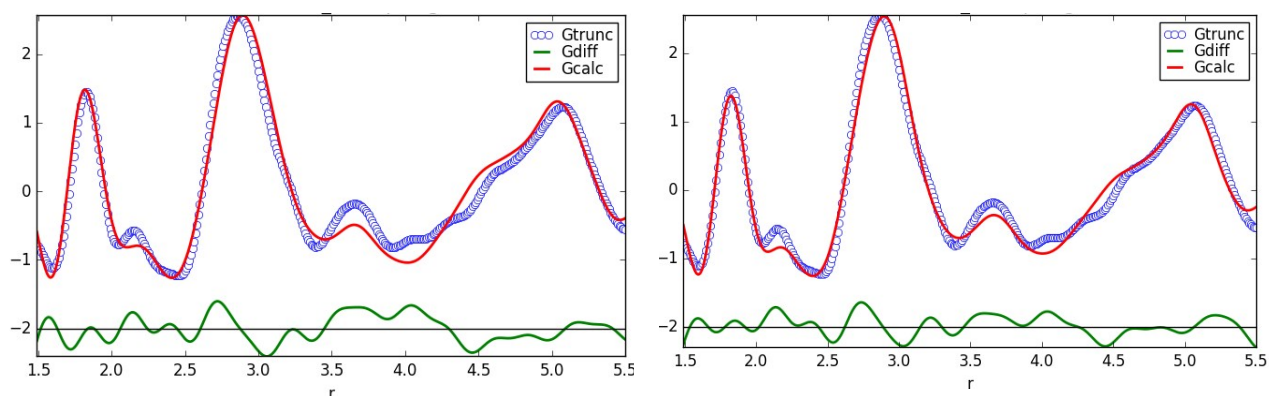


Figure S10. PDF modelling using the hybrid model up to 5.5 Å (left, $R_w=0.20$) and allowing the O displacement to form 5-fold coordinated M1 polyhedra (right, $R_w=0.15$).

In this case the distorted model improved the fit, especially with respect to the distance range between 3.5 and 5.0 Å. Still, the fit is not very good because other sources of disorder have to be explicitly described, for example the occupation of M1 and M2 sites, which here is described only via fractional occupancies, while the actual position of the coordinated O ions would change depending on which site is locally occupied. However, this very simple model, which involves the addition of only two further parameters, leads to some non negligible correlations between parameters (between atomic coordinates of O1, M2 and Ba2 sites). More detailed modelling would necessarily required independent coordinates for other ions, likely improving the fit, but increasing the probability to extract unphysical results.

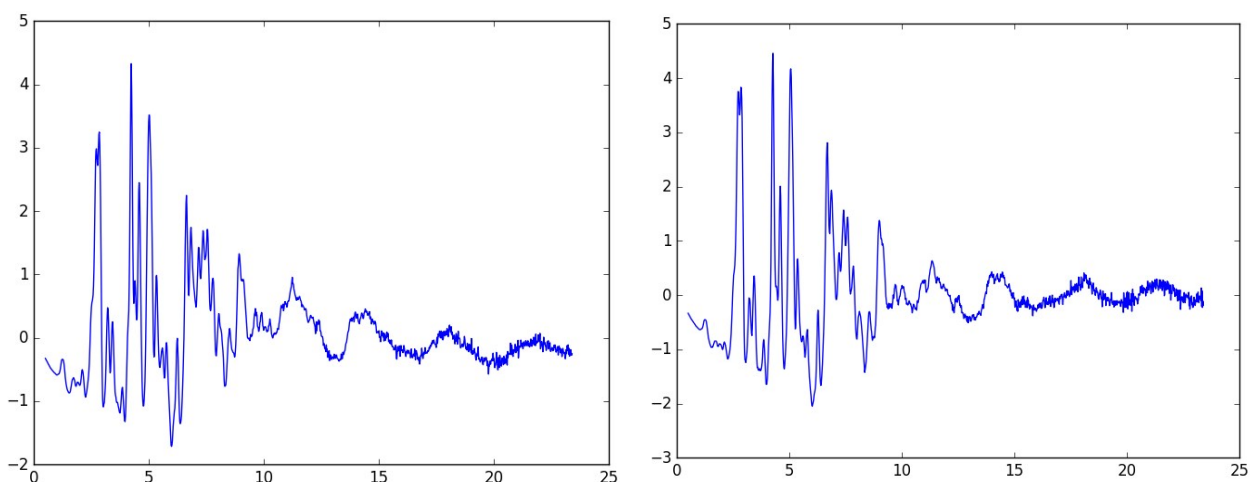
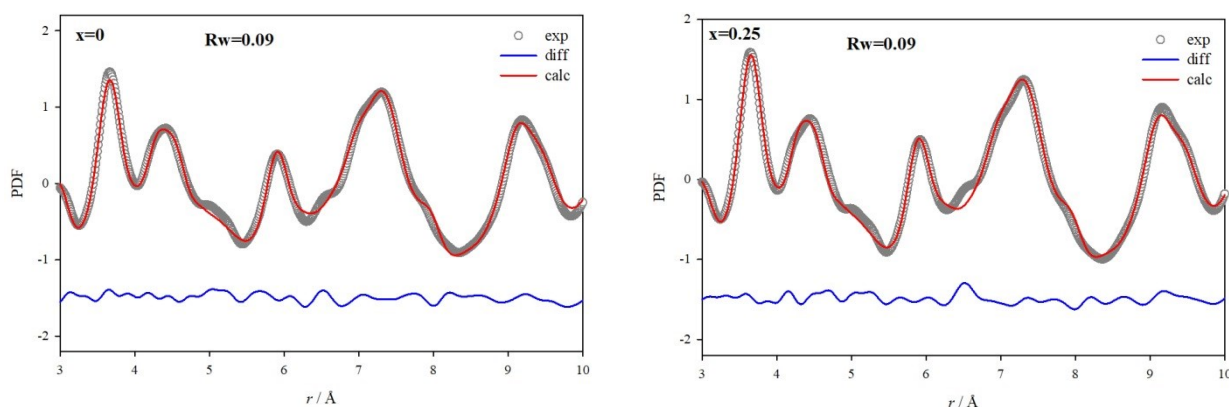


Figure S11: Experimental $F(Q)$ from NPD of Ba₃MoNbO_{8.5} (left) and Ba₃WNbO_{8.5} (right).



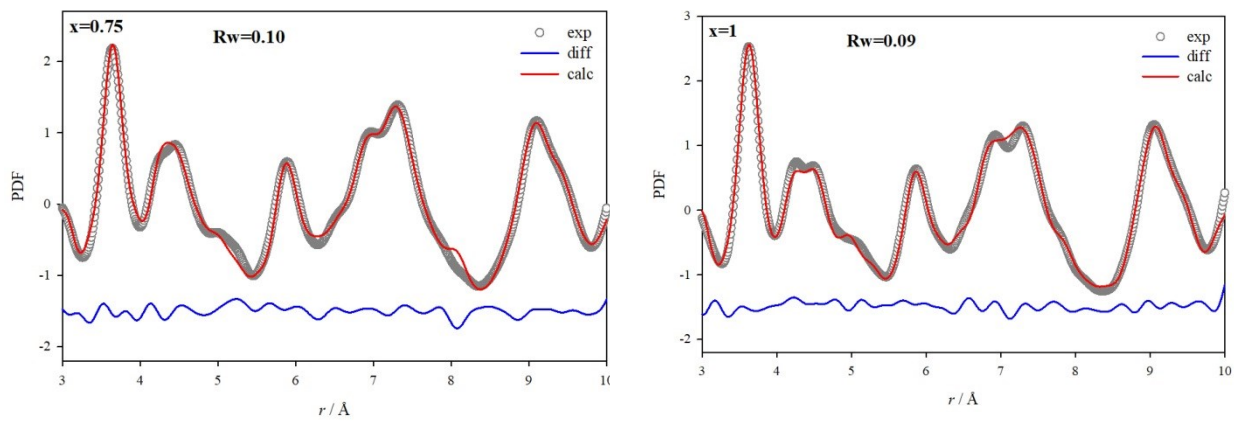
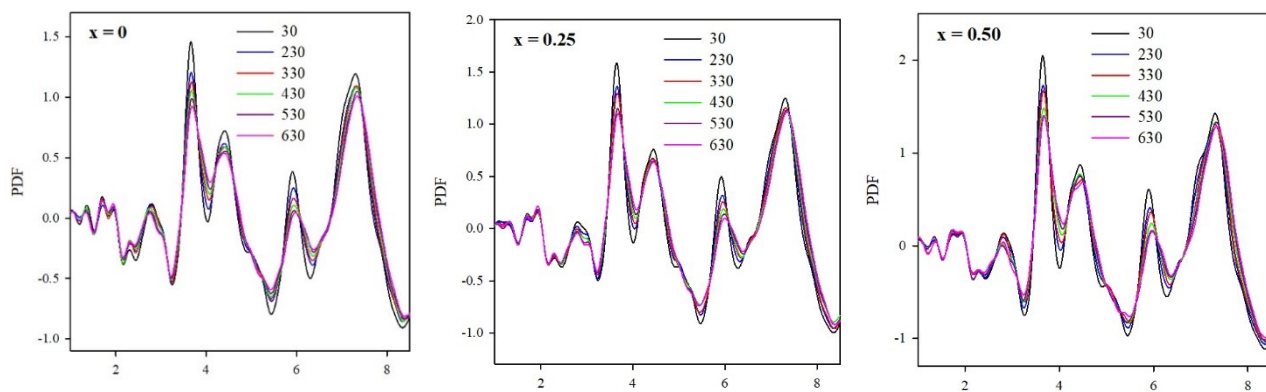


Figure S12. PDF refinements using a palmierite and 9R-palmierite two-phase model at RT up to 10 Å for different compositions.



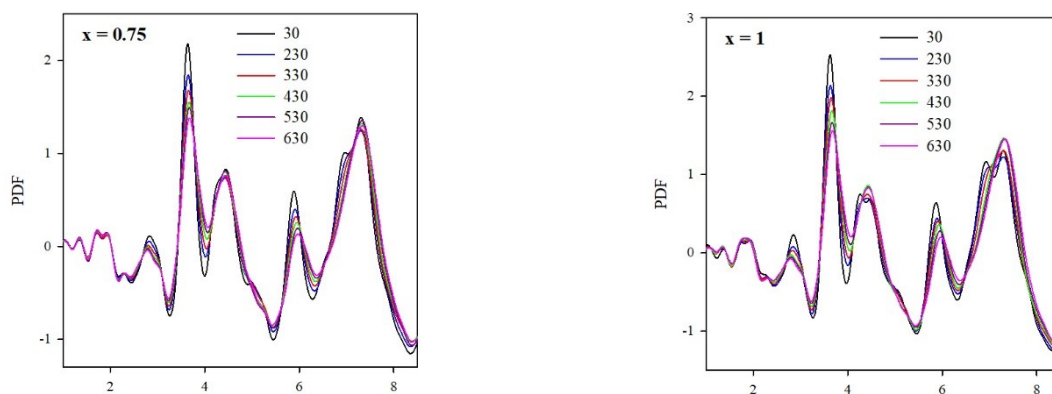


Figure S13. Temperature resolved experimental X-PDF curves for all the compositions investigated.

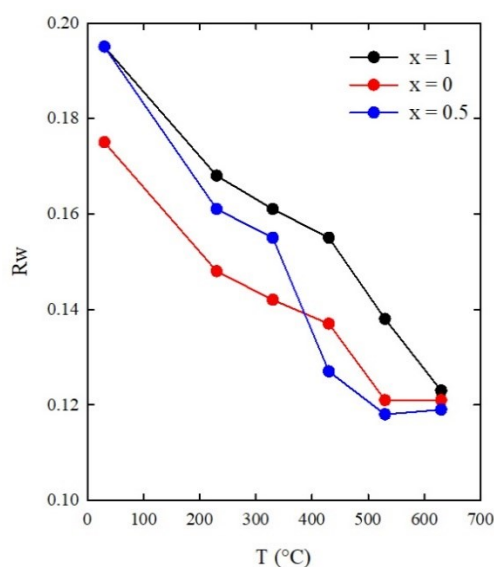


Figure S14. PDF fit residual of high temperature X-PDF using a single HA model.

Text S3: X-PDF refinement strategy

Single phase refinements were performed using the HA model proposed by Auckett. [10] Oxygen occupancies were fixed to 0.5 for O2 and 0.166 for O3 as their refinement did not lead to any fit improvement. This is consistent with the low weight of O-related parameters in the $\text{Ba}_3\text{Mo}_{1-x}\text{W}_x\text{NbO}_{8.5}$ system using X-rays. Isotropic *msd* were employed.

As to the two-phase model, we used the structures and the occupancies of palmierite and R9 as reported in Table 1 of the main text. Interestingly, attempts to refine the *z* coordinate of M2 site out of the special (0, 0, 0.5) position led to a value very close to 0.5. As we noticed that attempts to use anisotropic *msd* with the single

HA model led to displacements much larger along the c direction - and this is consistent with many reports - we used a different value of c lattice parameters for R9 and palmierite. In order to reduce the total number of refined parameters, we refined a single scale factor (an overall scale factor is kept fixed, only the scale factor of a single phase is refined while the other is modify to adds to one) and we constrained the msd of same atomic species of the two phases to the same values (a single parameter for M1 and M2, another parameter for all O sites). Moreover, the parameter accounting for the correlated motion is set the same for the two phases.